# An efficient approach for locating the critical slip surface in slope stability analyses using a real-coded genetic algorithm

**Yu-Chao Li, Yun-Min Chen, Tony L.T. Zhan, Dao-Sheng Ling, and Peter John Cleall**

**Abstract:** A real-coded genetic algorithm is employed to develop a search approach for locating the noncircular critical slip surface in slope stability analyses. Limit equilibrium methods and the finite-element-based method are incorporated with the proposed search approach to calculate the factor of safety. Geometrical and kinematical compatibility constraints are established based on the features of slope problems to prevent slip surfaces from being unreasonable. A dynamic bound technique is presented to improve the search performance with more effective exploration within the solution domain. A number of examples are investigated that demonstrate the proposed search approach to be efficient in yielding accurate solutions to practical slope stability problems. The proposed search approach is stable and highly correlated with the results of independent analyses. Furthermore, this paper demonstrates the successful application of a real-coded genetic algorithm to noncircular critical slip surface search problems.

*Key words:* genetic algorithm, critical slip surface, slope stability analysis, factor of safety.

**Résumé :** Un algorithme génétique est utilisé pour développer une approche de recherche afin de localiser la surface critique de glissement non-circulaire dans les analyses de stabilité de pente. Les méthodes de l'équilibre limite et une méthode basée sur les éléments finis ont été incorporées à l'approche de recherche proposée dans le but de calculer le facteur de sécurité. Les contraintes de compatibilité géométriques et cinématiques sont établies selon les caractéristiques des problèmes de pente, et ce afin de prévenir que les surface de glissement deviennent déraisonnables. Une technique dynamique est présentée pour améliorer la performance de la recherche avec des explorations plus efficace à l'intérieur du domaine de la solution. Plusieurs exemples sont investigués afin de démontrer que l'approche proposée est efficace pour donner des solutions précises aux problèmes pratiques de stabilité de pente. L'approche de recherche proposée s'avère être stable, avec une forte corrélation entre les résultats d'analyses indépendantes. De plus, cet article démontre l'application d'un algorithme génétique dans les problèmes de recherche des surfaces critiques de glissement non-circulaires.

*Mots-clés :* algorithme génétique, surface critique de glissement, analyse de stabilité de pente, facteur de sécurité.

[Traduit par la Rédaction]

## Introduction

A full slope stability analysis generally comprises evaluation of the factor of safety ($F_s$) for the given slip surfaces and determination of the critical slip surface, which is associated with the global minimum factor of safety ($F_{s_{min}}$). Several methods based on the concept of limit equilibrium (Janbu 1954; Bishop 1955; Morgenstern and Price 1965; Spencer 1967; Sarma 1973) are widely employed in practice to calculate the factor of safety in slope stability analyses because of their simplicity and ease of use. In recent years, a method that obtains the normal and shear stresses acting along the slip surface from finite-element-based stress analysis (Yamagami and Ueta 1988; Zou et al. 1995; Farias and Naylor 1998; Fredlund and Scoular 1999; Pham and Fredlund 2003) has drawn much attention, since it needs no assumptions relating to the inter-slice forces and the equation to calculate $F_s$ is linear (Pham and Fredlund 2003).

To determine the critical slip surface, approaches initially adopted pattern search schemes to identify circular or logarithmic spiral critical slip surfaces. However, these approaches often fail to capture the critical failure mode for nonhomogeneous slopes. For slopes with complex profiles, the function of $F_s$ is normally nonsmooth and (or) nonconvex (Cheng 2003) and has multiple minima (Chen and Shao 1988; McCombie and Wilkinson 2002) with respect to the location of the slip surface over the solution domain. This leads to a challenging problem when trying to identify the global $F_{s_{min}}$. Calculus-based methods (Baker 1980; Celestino

Received 2 March 2009. Accepted 28 September 2009. Published on the NRC Research Press Web site at cgj.nrc.ca on 25 June 2010.

**Y.-C. Li.** MOE Key Laboratory of Soft Soils and Geoenvironmental Engineering, Department of Civil Engineering, Zhejiang University, Anzhong Building, Zhijinggang Campus, 388 Yuhangtang Road, Hangzhou, 310058, P.R. China; Geoenvironmental Research Centre, Cardiff School of Engineering, Cardiff University, Queens Buildings, The Parade, Newport Road, Cardiff CF24 3AA, Wales, UK.
**Y.-M. Chen,[1] T.L.T. Zhan, and D.-S. Ling.** MOE Key Laboratory of Soft Soils and Geoenvironmental Engineering, Department of Civil Engineering, Zhejiang University, Anzhong Building, Zhijinggang Campus, 388 Yuhangtang Road, Hangzhou, 310058, P.R. China.
**P.J. Cleall.** Geoenvironmental Research Centre, Cardiff School of Engineering, Cardiff University, Queens Buildings, The Parade, Newport Road, Cardiff CF24 3AA, Wales, UK.

[1]Corresponding author (e-mail: chenyunmin@zju.edu.cn).

**Table 1.** Functions for describing the geological conditions.

| Function | Physical meaning |
|---|---|
| $y = t(x)$ | Slope surface |
| $y = l_i(x)$ | Discontinuous surfaces in layered soils |
| $y = h(x)$ | Bottom boundary of the solution domain (stiff soil or rock) |
| $y = w(x)$ | Phreatic line |
| $y = s(x)$ | Slip surface |

**Fig. 1.** Formulation of slope stability problem.

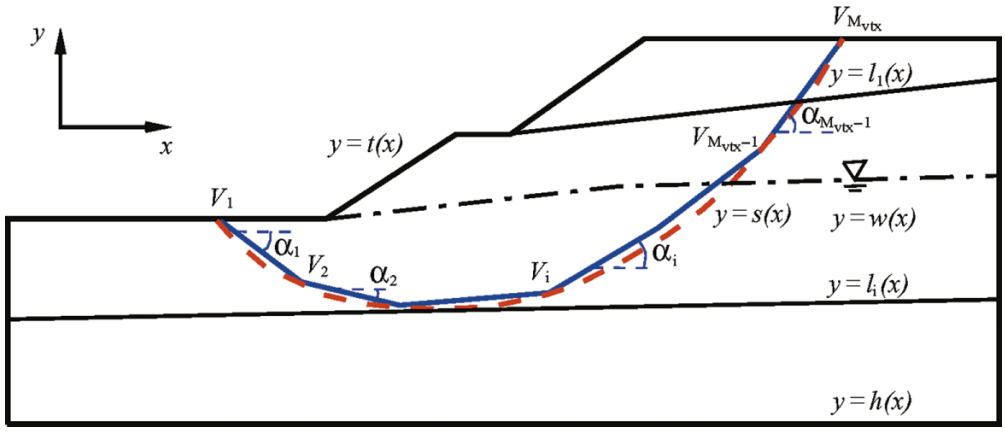


and Duncan 1981; Narayan et al. 1982; Arai and Tagyo 1985; Li and White 1987; Chen and Shao 1988; Bardet and Kapuskar 1989; Menon et al. 2001) can lead to identification of a false critical slip surface due to multiple minima over the solution domain (McCombie and Wilkinson 2002). Although more traditional random search techniques (Boutrup and Lovell 1980; Siegel et al. 1981; Chen 1992; Greco 1996; Jusein Malkawi et al. 2001*a*, 2001*b*) are often able to obtain a satisfactory solution, their success is quite by chance and normally requires a large number of possible slip surfaces to be generated and checked to enhance the probability of finding the critical slip surface. For approaches with an artificial grid discretization of the search domain, such as the critical slip field method (Zhu 2001) and the dynamic programming method (Pham and Fredlund 2003), the computing time and solution error are strongly related to the degree of discretization of the grid. Sarma and Tan (2006) proposed a search method based on the limit equilibrium technique (Sarma 1979) utilizing both a kinematical compatibility criterion and a stress acceptability criterion, the latter of which was regarded as a prerequisite to derive a system of nonlinear equations to determine the slip surface slice-by-slice upwards; however, this approach cannot reliably account for the resultant distortion.

Some modern heuristic optimization techniques have been employed in recent years in slope stability analyses to search for the noncircular critical slip surfaces. For example, Goh (1999) and Zolfaghari et al. (2005) incorporated a binary simple genetic algorithm (GA) with the multiple-wedge method and Morgenstern–Price method, respectively. However, Cheng et al. (2007) reported much lower minimum values of $F_s$ for two of the examples in Zolfaghari et al. and pointed out that the simple GA Zolfaghari et al. proposed appeared to be affected by the presence of a local minimum. Cheng (2003) and Cheng et al. (2007) applied simulated annealing and modified particle swarm optimization methods, respectively, to slope stability analyses and reported solution times of about 5 min on a PII 300 MHz personal computer (Cheng 2003) with tens of thousands of trials required (Cheng 2003; Cheng et al. 2007).

In this paper, a real-coded GA, which has been found to be more suitable for continuous problems than the binary GA (Hrstka and Kucerova 2004), is employed to develop an efficient search approach to locate noncircular critical slip surfaces in slope stability analyses. Geometrical and kinematical compatibility constraints are established according to the features of slope stability problems and included in the proposed approach to avoid unreasonable slip surfaces. A dynamic bound technique is presented to define the exploration range of slip surfaces. Six examples are investigated to demonstrate the efficiency of the proposed approach in solving practical slope stability problems. Another primary objective of this paper is to assess the potential application of a real-coded GA to noncircular critical slip surface search problems.

## Formulation of the problem

Two-dimensional slope stability problems are considered in this paper. Several mathematical functions to describe the geological profile and the slip surface for a general case are defined in Table 1 and illustrated in a generalized schematic diagram of the problem in Fig. 1.

### Slip surface approximation and function of the factor of safety

In slope stability analyses, noncircular slip surfaces are usually approximated by a polyline connecting $M_{vtx}$ vertices, i.e., $V_1(x_1, y_1)$, $V_2(x_2, y_2)$, …, $V_i(x_i, y_i)$, …, $V_{M_{vtx}}(x_{M_{vtx}}, y_{M_{vtx}})$, as shown in Fig. 1. Here, the order of the vertices is from downhill to uphill. A mirror operator is needed to transform the

**Fig. 2.** Unacceptable "broken" slip surface.

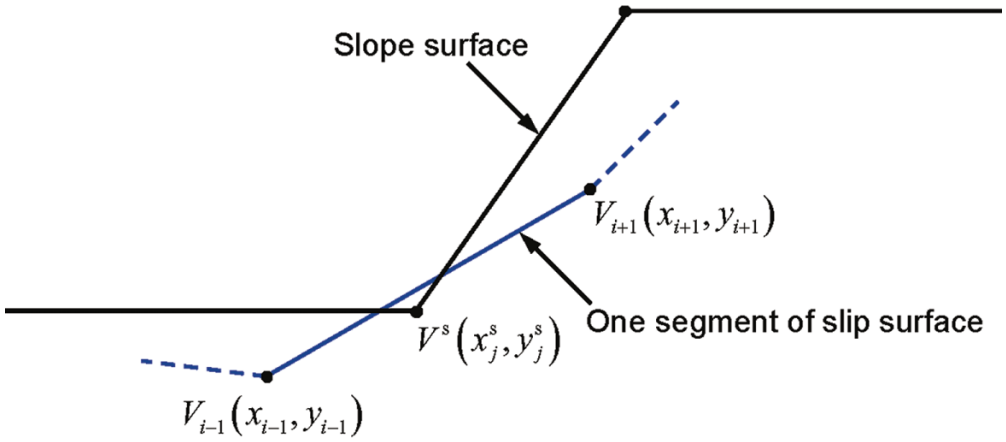


slope beforehand if the slope direction of movement is opposite to that shown in Fig. 1, in which $\alpha_i$ is the inclination angle, from the horizontal, of the $i$th segment of the slip surface, with a positive angle corresponding to counterclockwise rotation. Therefore, one slip surface can be represented by a vector

$$[1] \qquad \boldsymbol{s}_{M_{\text{vtx}}} = \{x_1, y_1, x_2, y_2, \ldots, x_i, y_i, \ldots, x_{M_{\text{vtx}}}, y_{M_{\text{vtx}}}\}^{\text{T}}$$

The factor of safety can be regarded as being a function of the slip surface ($\boldsymbol{s}_{M_{\text{vtx}}}$). The process of locating the critical slip surface can therefore be mathematically formulated as an optimization problem of minimizing the objective function $F_s$ with respect to $\boldsymbol{s}_{M_{\text{vtx}}}$ over the solution domain.

### Geometrical and kinematical compatibility constraints for slip surfaces

To avoid impossible or unreasonable slip surfaces, it is necessary to ensure that the slip surfaces considered meet the following geometrical and kinematical compatibility constraints:

(1) the $x$ ordinates of the vertices along the slip surface must be in monotone order;
(2) the two end vertices of the slip surface must be on the slope surface;
(3) all non-end vertices must be within the solution domain; and
(4) "broken" slip surfaces, as shown in Fig. 2, must be eliminated by ensuring that slope surface vertices, i.e., $V^s(x_j^s, y_j^s)$, are above the slip surface.

In terms of kinematics, the slip surface should be concave upward (Husein Malkawi et al. 2001*b*; Cheng 2003; Sarma and Tan 2006; Cheng et al. 2007) when the slope fails, that is,

$$[2] \qquad \alpha_i < \alpha_{i+1} \quad i = 1, 2, \ldots, M_{\text{vtx}} - 2$$

It is of interest to note that this constraint is not a prerequisite to the proposed approach and can be neglected if a slope with an exceptional geological profile is considered. However, this would typically result in a much longer search because many unreasonable slip surfaces might be considered.

The Rankine failure angle with respect to the direction of the third primary stress is $45^\circ+\phi/2$, where $\phi$ is the friction angle of the soil. Thus, $\alpha_1$ can be limited in the range of (–45°, 0°) and $\alpha_{M_{\text{vtx}}-1}$ (the inclination angle of the ($M_{\text{vtx}}$–1)th segment of the slip surface) in the range of (0°, 60°) if $\phi$ is less than 30°. The bound angles, however, can be specified with other values, if necessary, according to the geological profile and soil properties (as shown in example 3 of the Application section).

## Real-coded genetic algorithm

The GA technique, which was described by Holland (1975), is an adaptive heuristic search procedure inspired by ideas of evolution, natural selection, and genetics. The basic principles of the binary GA technique are described in detail in Goh (1999) and Zolfaghari et al. (2005), and the focus of this section is to outline the specific features of the proposed approach.

*Solution representation* — For continuous problems whose variables have a continuous rather than discrete distribution in the solution domain, a real-value representation of the potential solution is obviously more reasonable and simpler than a binary representation. Here, the vector $\boldsymbol{A}^j = \{a_1^j, a_2^j, \ldots, a_i^j, \ldots, a_{n-1}^j, a_n^j\}^{\text{T}}$ is used to represent an $n$ variable real-value solution to a continuous optimization problem, where $a_i$ is a real variable, and the superscript $j$ is the serial number of an individual solution in the population.

*Parent selection* — A number of selection strategies for GA have been proposed, such as uniformly distributed random selection, roulette wheel selection (Holland 1975), and tournament selection (Goldberg and Deb 1991). Linear-ranking selection (Eiben and Smith 2003) is adopted in this paper to select two of the existing solutions as parents for breeding children. This selection scheme can preserve a constant selection pressure by sorting the solutions based on fitness and then allocating selection probabilities to them according to their rank.

*Crossover* — Single arithmetic crossover (Eiben and Smith 2003) with a specified probability ($r_{\text{crs}}$) is performed for each variable in this paper. For two solutions $\boldsymbol{A}^p$ and $\boldsymbol{A}^q$ selected as parents to breed children, if the variable $a_k$ is picked up for crossover, the crossover operator acts as follows:

$$[3] \qquad \begin{cases} \boldsymbol{A}^p = \{a_1^p, a_2^p, \ldots, a_k^p, \ldots, a_{n-1}^p, a_n^p\}^{\text{T}} \\ \boldsymbol{A}^q = \{a_1^q, a_2^q, \ldots, a_k^q, \ldots, a_{n-1}^q, a_n^q\}^{\text{T}} \end{cases} \rightarrow$$

$$\begin{cases} \boldsymbol{A}^{p'} = \{a_1^p, a_2^p, \ldots, \eta a_k^p + (1-\eta)a_k^q, \ldots, a_{n-1}^p, a_n^p\}^{\text{T}} \\ \boldsymbol{A}^{q'} = \{a_1^q, a_2^q, \ldots, (1-\eta)a_k^p + \eta a_k^q, \ldots, a_{n-1}^q, a_n^q\}^{\text{T}} \end{cases}$$

**Fig. 3.** Generation of initial slip surfaces.

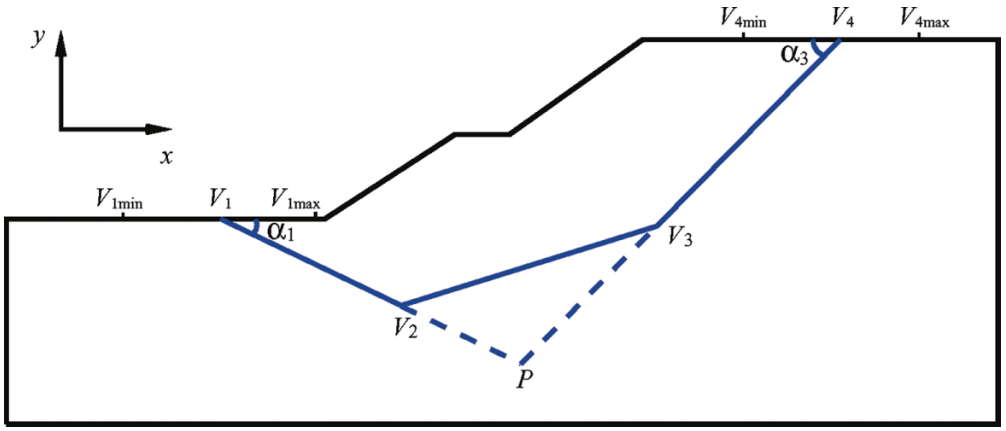


where $A^{p'}$ and $A^{q'}$ are the child solutions after crossover, and $\eta$ is a parameter for controlling crossover rate and is usually chosen at random over (0, 1).

*Mutation* — Uniform mutation (Eiben and Smith 2003) with a specified probability ($r_{mut}$) is performed for each variable in this paper. For a solution $A^j$, if the variable $a_k$ is picked up for mutation, the mutation operator acts as follows:

$$[4] \quad A^j = \{a_1^j, a_2^j, \ldots, a_k^j, \ldots, a_{n-1}^j, a_n^j\}^T \rightarrow A^{j'} = \{a_1^j, a_2^j, \ldots, a_k^{j'}, \ldots, a_{n-1}^j, a_n^j\}^T, \quad a_k^{j'} \in [a_{k_{min}}, a_{k_{max}}]$$

where $A^{j'}$ is the solution after mutation; and $a_k^{j'}$ is drawn randomly within its domain given by a bound of $a_{k_{min}}$ and $a_{k_{max}}$, the lower and upper boundaries, respectively, for $a_k$.

*Survivor selection* — After crossover and mutation, tournament selection (Goldberg and Deb 1991) is applied with elitism (de Jong 1975) to select the survivors from parents and children. In this study, the fittest solution is selected first to prevent the loss of the current best solution. Then, several solutions are picked up randomly, and the fittest (i.e., the solution with the lowest $F_s$) among them is selected as the survivor. It should be noted that one solution is selected as a survivor no more than once.

## Search process

The framework of the real-coded GA implemented in this study to locate the critical slip surface is illustrated in Fig. A1. The geometrical and kinematical compatibility constraints are checked after the crossover and mutation operators to eliminate unacceptable child slip surfaces. The dynamic termination condition proposed by Cheng et al. (2007) is adopted here. With this technique, the search process is stopped if the improvement of the lowest $F_s$ is less than a specified relative difference ($\varepsilon_{term}$) for a number of generations ($M_{NI\_term}$) after a minimum number of generations ($M_{term}$) have been assessed.

The following techniques are developed here to improve the performance of the search algorithm in locating the critical slip surface.

### Generation of initial slip surfaces

As with other random optimization techniques, such as the Monte Carlo method (Greco 1996) and the modified particle swarm optimization method (Cheng et al. 2007), the GA method requires a number of initial slip surfaces to be generated. Here, $M_{slip}$ is defined as the number of the slip surfaces in the population. The technique presented by Boutrup and Lovell (1980) is modified in this paper to generate initial slip surfaces with four vertices so that the position of the end vertices is restricted to a defined range of locations. The end vertices, $V_1$ and $V_4$, are generated randomly within the range of ($V_{1min}$, $V_{1max}$) and ($V_{4min}$, $V_{4max}$), respectively, as illustrated in Fig. 3. The bound values, i.e., $V_{1min}$, $V_{1max}$, $V_{4min}$, and $V_{4max}$, are defined beforehand according to the geological profile and soil properties. Wider ranges can be specified for the cases with greater uncertainty.

### Dynamic bounding technique for the vertices of slip surfaces

For the real-coded GA, upper and lower bounds for the variable are required when the mutation operator is performed. Cheng (2003) presented a dynamic bound scheme for the control variables of the simulated annealing approach. However, this approach may result in a high rejection rate of the mutation by the geometrical and kinematical compatibility constraints, and thus the explorative function of mutation may be weakened significantly. To overcome this limitation, an improved dynamic bounding technique is proposed here that restricts the effective exploration range for the vertices of the slip surfaces, as illustrated in Fig. 4. The technique is described in the following for the two cases of (1) end vertices and (2) non-end vertices.

*Case 1: end vertices* $V_1$ and $V_{M_{vtx}}$ — If the $x$ coordinate is given, the $y$ coordinate can be obtained according to the slope-surface shape; therefore, only the upper and lower bounds for the $x$ coordinate are required. Here, $x_1+(x_2 - x_1)/2$ is used as the upper bound for $x_1$, and $x_{M_{vtx}} - (x_{M_{vtx}} - x_{M_{vtx}-1})/2$ as the lower bound for $x_{M_{vtx}}$. This approach prevents the end vertex from moving too quickly towards the next vertex in the horizontal direction. The other bound is defined as the $x$ coordinate of the intersection of the extension of $V_2V_3$ or $V_{M_{vtx}-2}V_{M_{vtx}-1}$ and the slope surface to ensure that the slip surface is concave upwards.

**Fig. 4.** Dynamic bounds for the vertices of slip surfaces.

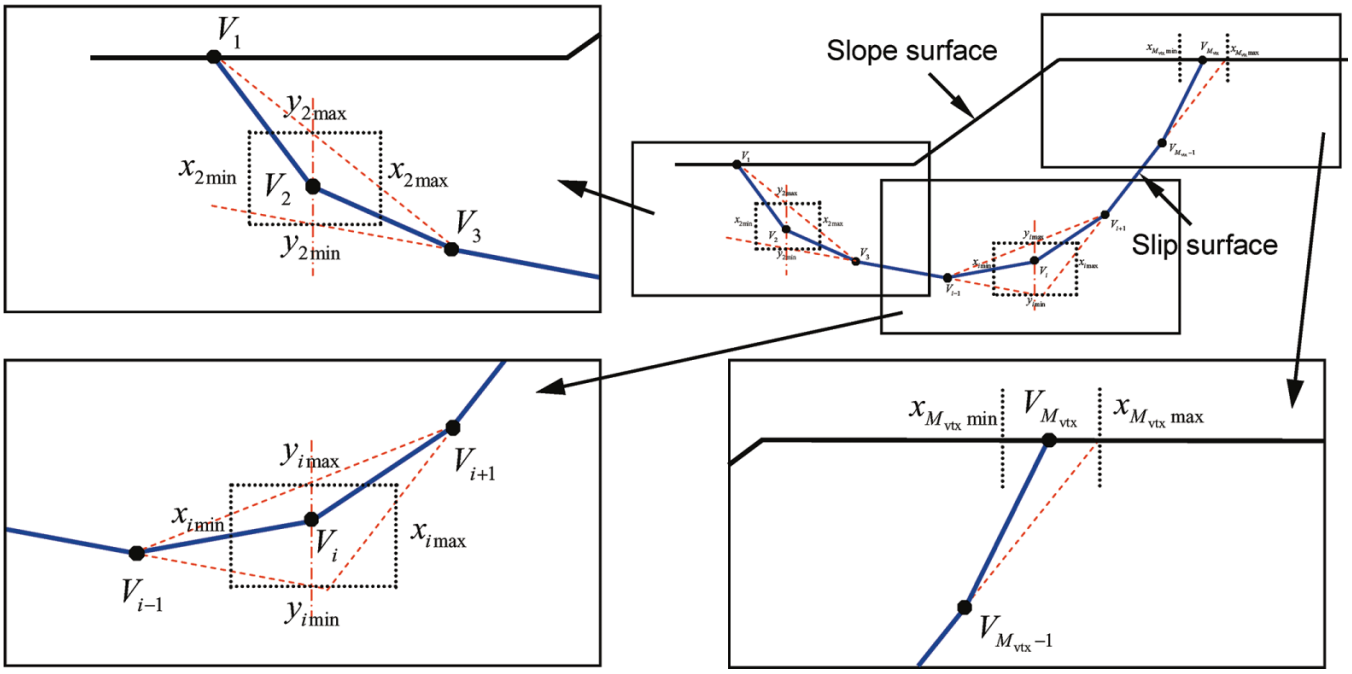


*Case 2: non-end vertices $V_i$ ($i$ = 2, 3,…, $M_{vtx}$–2, $M_{vtx}$–1)* — Following the approach adopted in case (1), $x_i$ is defined as being in the range of $[x_i-(x_i-x_{i-1})/2,\ x_i+(x_{i+1}-x_i)/2]$. The bound for $y_i$ is decided by the concave-upward constraint of the slip surface as follows:

$$[5a] \qquad y_{i_{\max}} = y_{i-1} + k_{i-1,i+1}(x_i - x_{i-1})$$

$$[5b] \qquad y_{i_{\min}} = \begin{cases} y_{i+1} + k_{i+1,i+2}(x_i - x_{i+1}), & i = 2 \\ \max[y_{i-1} + k_{i-2,i-1}(x_i - x_{i-1}),\ y_{i+1} + k_{i+1,i+2}(x_i - x_{i+1})], & i = 3, \ldots, M_{\text{vtx}} - 2 \\ y_{i-1} + k_{i-2,i-1}(x_i - x_{i-1}), & i = M_{\text{vtx}} - 1 \end{cases}$$

where $k_{i,j}$ is the slope of the line connecting $V_i$ and $V_j$.

The concave-upward constraint may not be satisfied if the vertex is within some corner parts of the dynamic bounds proposed previously, as illustrated in Fig. 4, although its probability is relatively small. Such cases can be avoided by applying the kinematical compatibility constraint after the mutation operator.

## Schemes for vertex addition and vertex-position modification

Obviously, the approximation error of the slip surfaces decreases with an increase in $M_{\text{vtx}}$. However, Li and White (1987) pointed out that too many vertices may result in interference among the vertices and hence may reduce the convergence rate. In the proposed method, the technique of adding vertices in succession proposed by Li and White (1987) is modified via inclusion of a dynamic addition condition. The search starts with a limited number of vertices, and then new vertices are successively introduced at the midpoints of the segments in either of the following two cases: (*i*) when the generation number $i_{\text{gen}}$ reaches $M_{\text{add}}$, which is a specified number of generations for adding vertices, if the best solution is continuing to significantly improve; and (*ii*) the improvement for the best solution is less than a specified relative difference $\varepsilon_{\text{add}}$ for $M_{\text{NI\_add}}$ generations, which is the maximum number of generations allowed with no significant improvement, even though $i_{\text{gen}}$ is less than $M_{\text{add}}$. The search is performed with slip surfaces defined by 4, 7, and 13 vertices, successively. This procedure has the merit of allowing large displacements in the initial search without interference between vertices and results in an accurate solution owing to the high number of vertices in the latter searches (Greco 1996).

To prevent the vertices from being too close to each other, a vertex-position modification scheme is proposed here and is conducted, if necessary, after mutation. For any three successive vertices $V_{i-1}$, $V_i$, and $V_{i+1}$, the coordinates of $V_i$ are modified by interpolation in the segment $V_iV_{i+1}$ if $(x_i-x_{i-1})/(x_{i+1}-x_i) < 1/3$, that is, the interval in the $x$ direction between $V_i$ and $V_{i+1}$ is more than three times that between $V_{i-1}$ and $V_i$. Similarly, the interpolation for $V_i$ in the segment $V_{i-1}V_i$ is performed if $(x_{i+1}-x_i)/(x_i-x_{i-1}) < 1/3$. In each case, the interpolation is performed to result in an $x$ coordinate value for $V_i$ of $(x_{i-1}+x_{i+1})/2$.

**Table 2.** Values recommended and used in this paper for the primary parameters.

| | Value recommended | Value used in this paper |
|---|---|---|
| $M_{slip}$ | $10 \sim 50$ | 20 (40 for example 4) |
| $r_{crs}$ | $0.5 \sim 0.9$ | 0.8 |
| $r_{mut}$ | $0.05 \sim 0.2$ | 0.15 |
| $M_{term}$ | $50 \sim 200$ | 100 |
| $M_{NI\_term}$ | $M_{term}/(10 \sim 20)$ | $M_{term}/10$ |
| $\varepsilon_{term}$ | $0.00002 \sim 0.0002$ | 0.00005 |
| $M_{add}$ | $M_{term}/3$, $2M_{term}/3$ | $M_{term}/3$, $2M_{term}/3$ |
| $M_{NI\_add}$ | $M_{term}/(6 \sim 20)$ | $M_{term}/6$ |
| $\varepsilon_{add}$ | $0.00002 \sim 0.0002$ | 0.00005 |

**Note:** For definitions, see List of symbols.

It is perhaps worth highlighting the differences between the proposed approach and the GA searching scheme presented by Goh (1999). These differences are summarized as follows:

(1) Real-value coding, rather than binary coding (Goh 1999), is adopted in the proposed approach to represent the coordinates of the vertices of slip surfaces, which are continuous in the search spaces. As such, binary search space discretization is not required, thereby avoiding the accuracy of results becoming highly dependent on the length of the binary string.

(2) Compared to Goh's (1999) use of a constant number of vertices of slip surfaces during the search process, the dynamic vertex addition scheme proposed here allows a more effective search with a coarse-grained resolution in the early stages and a finer grained resolution in the later stages.

(3) Compared with a specified static number of generations (Goh 1999), the dynamic termination condition (Cheng et al. 2007) adopted in the proposed approach can avoid losing better solutions due to early termination and ineffectual searches after the best solution has already been obtained.

(4) Other techniques proposed in this paper, such as dynamic bounding for the vertices of slip surfaces and vertex-position modification, further improve the search performance of the proposed approach.

The recommended values of the primary parameters in the proposed approach are listed in Table 2 together with those used in the following examples. The recommended value of $r_{mut}$ in this paper is greater than that used in many applications of GAs because the mutation operator used in the paper is not free and may be restricted later by kinematical compatibility constraints. Lastly, it has been found that the use of a constant value of the golden ratio $(\sqrt{5}-1)/2$ for $\eta$ results in an improved solution time and is therefore adopted here.

## Application

In this section, the proposed approach is used to investigate six examples and the results are compared with those in the literature. One of the key aspects of these examples is to assess the efficiency of the proposed approach in solving the problems.

The real-coded GA, like the simple binary GA (Goh 1999; Zolfaghari et al. 2005), the simulated annealing algorithm (Cheng 2003), and the modified particle swarm optimization technique (Cheng et al. 2007), belongs to the family of stochastic optimization techniques. As such, for each of these approaches, the results obtained in independent analyses with the same problem definition and parameters are typically different from each other. Also, the stability of the algorithm in finding the true or approximate solution is important, and thus it is of value to present the results of a number of independent analyses. In this study, a time-dependent seed is used to establish the starting point of the pseudorandom number generator in the computer code. Three independent analyses are performed for each example and the values of $F_{s_{min}}$ for all three analyses are reported. The slip surface with the lowest $F_{s_{min}}$ among the three analyses is regarded as the critical slip surface.

In examples 1–4, the algorithm for the Morgenstern–Price method (the Spencer method is also available if the constant inter-slice force function is used) proposed by Zhu et al. (2005) is used to calculate $F_s$, and the sliding mass is divided into 30 slices for each slip surface. It should be noted that the values of $F_s$ with unrealistic inter-slice forces (Morgenstern and Price 1965) are eliminated in the search process. In examples 5 and 6, a finite-element-based method is adopted for calculating $F_s$ (Yamagami and Ueta 1988; Zou et al. 1995; Farias and Naylor 1998; Fredlund and Scoular 1999).

The coordinates of the key points describing the geological layers and the phreatic lines (if any) in the six examples are listed in Table B1.

### Example 1

The first example considers a homogeneous slope, initially defined by Yamagami and Ueta (1988), and is shown in Fig. 5 with its soil properties indicated. This problem has been considered by a number of researchers, and the results obtained in those studies are listed in Table 3.

The minimum factors of safety from three independent analyses of the proposed approach are 1.327, 1.327, and 1.329. A comparison with the results given in Table 3 shows that these values are very close to those obtained using the Monte Carlo technique (Greco 1996) and the modified particle swarm optimization technique (Cheng et al. 2007). The critical slip surface for the analysis with the lowest $F_{s_{min}}$ is in good agreement with those reported in Greco (1996) and Cheng et al. (2007), as shown in Fig. 5. For completeness, the exact locations of the critical slip surfaces obtained using the proposed approach for each of the examples investigated in this paper are given in Table C1.

As listed in Table 3, the number of different possible slip surfaces considered, which indicates the efficiency of the search approach, for analysis with the lowest $F_{s_{min}}$ is 2020, which is less than one tenth of the value reported for the modified particle swarm optimization approach (Cheng et al. 2007). Greco (1996) did not provide equivalent information for the Monte Carlo technique; however, a computer program implementing Greco approach has been developed for a qualitative comparison and the number of solutions required is typically $5 \sim 10$ times that required for the proposed approach. Furthermore, the Monte Carlo technique performs a larger number of ineffective modifications of vertices, which cause most of the computing load of this technique and greatly reduce its efficiency owing to a lack of effective bounding techniques for the vertices of slip surfaces. The computing time required for the proposed approach for the whole search process is 3.43 s for analysis

**Fig. 5.** Cross section and critical slip surfaces for example 1.

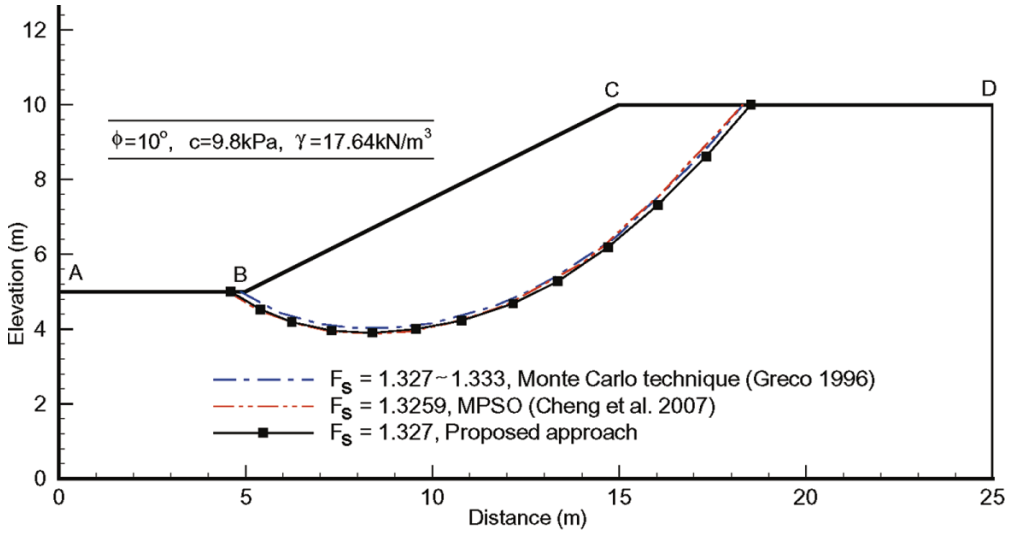


with the lowest $F_{s_{min}}$ on an IBM T60 laptop with Core Duo 1.66 GHz Genuine Intel(R) central processing unit (CPU) and 512 Mb random access memory (RAM).

The convergence curve for the analysis with the lowest $F_{s_{min}}$ is shown in Fig. 6. The lowest $F_s$ drops dramatically just after the first vertex addition (from 4 to 7 vertices). It remains almost unchanged for a number of generations before the second vertex addition (from 7 to 13 vertices). A fine search near the current best solution occurs in the latter stage and then $F_{s_{min}}$ is obtained, according to the convergence criteria. The convergence curve indicates that the proposed modified technique of adding vertices during the search process results in a step-by-step improvement in the solution.

To assess the impact of more vertices, another analysis was performed that allows a further increase of up to 25 vertices to define the slip surface. The number of generations for adding vertices $M_{add} = M_{term}/4$, $M_{add} = M_{term}/2$, and $3M_{term}/4$ and $M_{NI\_add} = M_{term}/8$ is adopted with other parameters remaining unchanged. The convergence curve for this analysis, also shown in Fig. 6, is quite similar to that of the 13-vertex analysis and results in a slightly lower $F_{s_{min}}$ of 1.326; however, this is an improvement of less than 0.1%. Based on a number of parametric analyses using the proposed approach, this limited impact of moving to a higher number of vertices is typical; and consequently, the scheme of adding up to 13 vertices is adopted in the following examples.

**Fig. 6.** Convergence process of the lowest factor of safety for example 1.

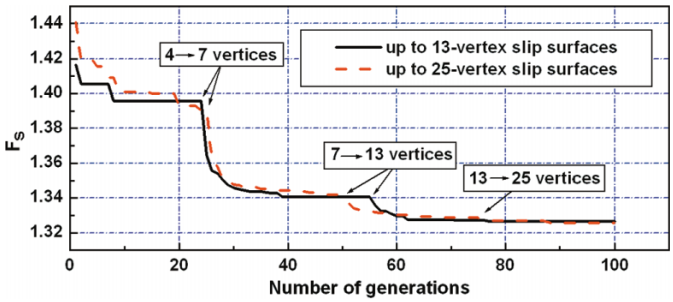


## Examples 2–4

Examples 2 and 3 were originally presented by Zolfaghari et al. (2005); and the geological profiles and soil properties are shown in Figs. 7 and 8, respectively. Zolfaghari et al. analyzed these two examples using the simple binary GA technique with the Morgenstern–Price method (with a sine function for the inter-slice forces being adopted) and obtained $F_{s_{min}}$ values of 1.24 and 1.48 for examples 2 and 3, respectively. As listed in Table 3, Cheng et al. (2007) reported much lower $F_{s_{min}}$ values for these two examples using the modified particle swarm optimization with the Spencer method.

Here, the two examples are reanalyzed using the Morgenstern–Price method to calculate $F_s$ following Zolfaghari et al. (2005); however, the proposed real-coded GA approach is adopted as the search algorithm instead of the simple binary GA. It should be noted that a bound of $-10^\circ < \alpha_1 < 30^\circ$, on the view of the slope direction shown in Fig. 1, is set for $\alpha_1$ in example 2 based on the gradient of the weak layer, i.e., layer 3. As listed in Table 3, $F_{s_{min}}$ values of 1.113 and 1.335 are obtained by the proposed approach for examples 2 and 3, respectively. These values are significantly lower than those presented by Zolfaghari et al. To compare with the results of Cheng et al. (2007), additional analyses have been conducted by the proposed search approach using the Spencer method to calculate $F_s$. Minimum factors of safety of 1.114 and 1.336 are obtained for examples 2 and 3, respectively. These values are very similar to those determined using the Morgenstern–Price method and slightly lower than those reported for the modified particle swarm optimization approach by Cheng et al.

The critical slip surfaces obtained by the proposed approach are shown in Figs. 7 and 8 along with those reported in the literature. For both examples, the critical slip surfaces obtained by the proposed approach with Morgenstern–Price and Spencer methods are strongly correlated. Their modes are similar to those reported by Cheng et al. (2007). However, the difference between these critical slip surfaces and those obtained by Zolfaghari et al. (2005) is noticeable. A smaller portion of the critical slip surfaces obtained by Zolfaghari et al. lies within the weak layer of the system (particularly for example 3), and thus much higher $F_{s_{min}}$ values could be ex-

**Table 3.** Minimum factors of safety for the examples investigated.

| Search approach | Method for calculating factor of safety ($F_s$) | Minimum value of factor of safety ($F_{s_{min}}$) | No. of slip surfaces considered | Computing time (s) |
|---|---|---|---|---|
| **Example 1** | | | | |
| BFGS, DFP, Powell (Yamagami and Ueta 1988) | Spencer | 1.338 | Unknown | Unknown |
| Simplex (Yamagami and Ueta 1988) | Spencer | 1.339 ~ 1.348 | Unknown | Unknown |
| Pattern search (Greco 1996) | Spencer | 1.327 ~ 1.330 | Unknown | Unknown |
| Monte Carlo technique (Greco 1996) | Spencer | 1.327 ~ 1.333 | Unknown | Unknown |
| Monte Carlo technique (Husein Malkawi et al. 2001*a*) | Spencer | 1.238 (1.37)[a] | Unknown | Unknown |
| MPSO (Cheng et al. 2007) | Spencer (30 slices) | 1.3259 | 27 856 | Unknown |
| Real-coded GA (this paper) | Spencer (30 slices) | 1.327, 1.327, 1.329 | 2 020[b] | 3.43[b,c] |
| **Example 2** | | | | |
| Simple GA (Zolfaghari et al. 2005) | Morgenstern–Price | 1.24 | Unknown | Unknown |
| Critical acceleration (Sarma and Tan 2006) | Sarma | 1.091 | Unknown | Unknown |
| MPSO (Cheng et al. 2007) | Spencer (30 slices) | 1.1289 | 14 081 | Unknown |
| Real-coded GA (this paper) | Morgenstern–Price | 1.113, 1.115, 1.117 | 3 420[b] | 5.14[b,c] |
| Real-coded GA (this paper) | Spencer (30 slices) | 1.114, 1.116, 1.119 | 3 320[b] | 5.44[b,c] |
| **Example 3** | | | | |
| Simple GA (Zolfaghari et al. 2005) | Morgenstern–Price | 1.48 | Unknown | Unknown |
| MPSO (Cheng et al. 2007) | Spencer (30 slices) | 1.3490 | 14 874 | Unknown |
| Real-coded GA (this paper) | Morgenstern–Price | 1.335, 1.338, 1.339 | 2 460[b] | 3.43[b,c] |
| Real-coded GA (this paper) | Spencer (30 slices) | 1.336, 1.337, 1.337 | 2 520[b] | 3.62[b,c] |
| **Example 4** | | | | |
| MPSO (Cheng et al. 2007) | Spencer (30 slices) | 1.2006 | 15 153 | Unknown |
| Real-coded GA (this paper) | Spencer (30 slices) | 1.197, 1.201, 1.207 | 6 640[b] | 8.67[b,c] |
| **Example 5** | | | | |
| DP (Pham and Fredlund 2003) | Finite-element-based | 1.413 | Unknown | Unknown |
| SLOPE/W (Pham and Fredlund 2003) | Morgenstern–Price | 1.485 | Unknown | Unknown |
| Real-coded GA (this paper) | Finite-element-based | 1.393, 1.394, 1.396 | 2 260[b] | 3.47[b,c] |
| Real-coded GA (this paper) | Morgenstern–Price | 1.408, 1.410, 1.412 | 3 200[b] | 5.97[b,c] |
| **Example 6** | | | | |
| DP (Pham and Fredlund 2003) | Finite-element-based | 1.000 | Unknown | Unknown |
| SLOPE/W (Pham and Fredlund 2003) | Morgenstern–Price | 1.140 | Unknown | Unknown |
| Real-coded GA (this paper) | Finite-element-based | 0.997, 0.998, 1.000 | 2 140[b] | 4.74[b,c] |
| Real-coded GA (this paper) | Finite-element-based[d] | 1.028, 1.030, 1.036 | 2 420[b] | 5.53[b,c] |
| Real-coded GA (this paper) | Morgenstern–Price | 1.017, 1.021, 1.022 | 4 400[b] | 9.42[b,c] |

**Note:** BFGS, Broyden–Fletcher–Goldfarb–Shanno; DEP, Davidson–Fletcher–Powell; DP, dynamic programming; MPSO, modified particle swarm optimization; SLOPE/W, computer program.

[a]Recalculated by Cheng et al. (2007) for the same critical slip surface as that in Husein Malkawi et al. (2001*a*).

[b]Corresponds to analysis yielding the first value in $F_{s_{min}}$ column.

[c]Computing time on an IBM T60 laptop with Core Duo 1.66 GHz Genuine Intel(R) CPU and 512 Mb RAM.

[d]Elastoplastic finite-element analysis performed.

**Fig. 7.** Cross section and critical slip surfaces for example 2.

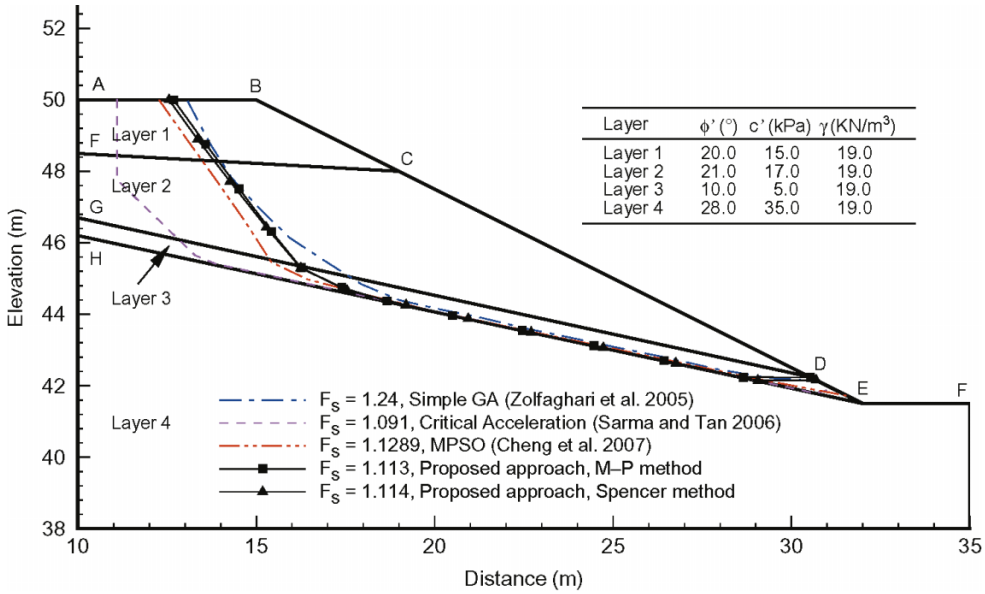


**Fig. 8.** Cross section and critical slip surfaces for example 3.

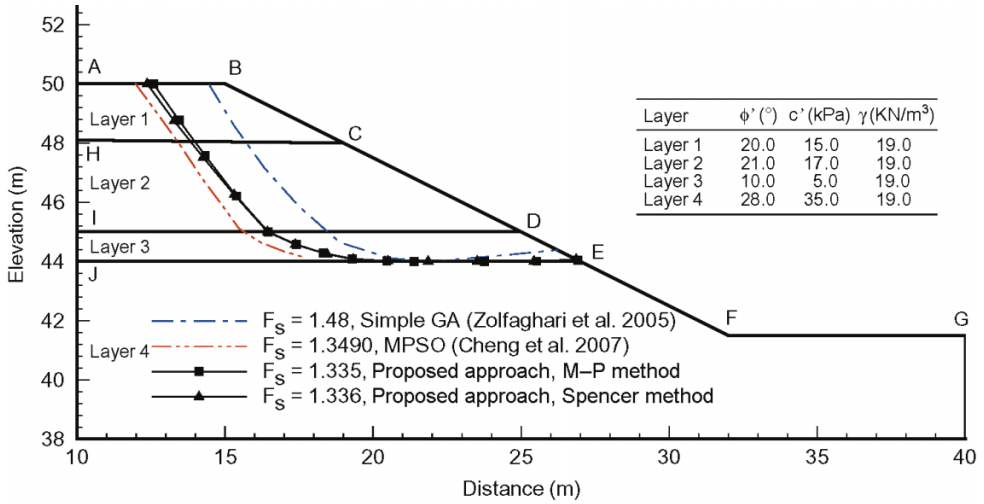


pected. Consequently, the simple binary GA proposed by Zolfaghari et al. failed to find the true solutions for these two examples based on both the comparisons of $F_{s_{min}}$ and the critical slip surface location. Cheng et al. speculated that this may be caused by the simple binary GA, proposed by Zolfaghari et al. being trapped by the presence of a local minimum.

The convergence process of the slip surfaces for example 2 (Morgenstern–Price method) is illustrated in Fig. 9. The $x$-coordinate ranges for the vertices $V_1$ and $V_4$ are specified as (10, 17) and (27, 34), respectively, when the initial slip surfaces are generated. The 20 initial four-vertex slip surfaces are distributed within the solution domain as shown in Fig. 9*a*. The exploration in the early stage appears to be quite effective and lowest $F_s$ drops from 1.480 to 1.179, as shown in Fig. 10. Although the slip surfaces are relatively coarse, before the addition of four to seven vertices, the slip surfaces already focus on the weak layers (Fig. 9*b*). The lowest $F_s$ has a distinct drop after the first vertex addition (Fig. 10), and then the slip surfaces explored near the current solution gradually tend towards the ultimate solution before the addition of 7 to 13 vertices (Fig. 9*c*). The final solution is obtained by a fine search (Fig. 10), and all the slip surfaces considered become almost identical when the search process is terminated (Fig. 9*d*). Both the convergence processes of the slip surfaces and the lowest $F_s$ show that the proposed approach achieves an excellent combination of a global explorative search in the early stages and a local fine search in the latter stages.

Furthermore, the proposed approach is much more efficient when compared with the modified particle swarm optimization (Cheng et al. 2007). The number of different possible slip surfaces considered by the proposed approach for examples 2 and 3, respectively, is less than one quarter and about one fifth of that of the modified particle swarm optimization solution, as listed in Table 3. It takes only 5.44 and 3.62 s for the proposed approach to solve examples 2 and 3, respectively, using the hardware configuration mentioned previously.

The thickness of the weak layer in example 2 was re-

**Fig. 9.** Convergence process of 20 slip surfaces for example 2.

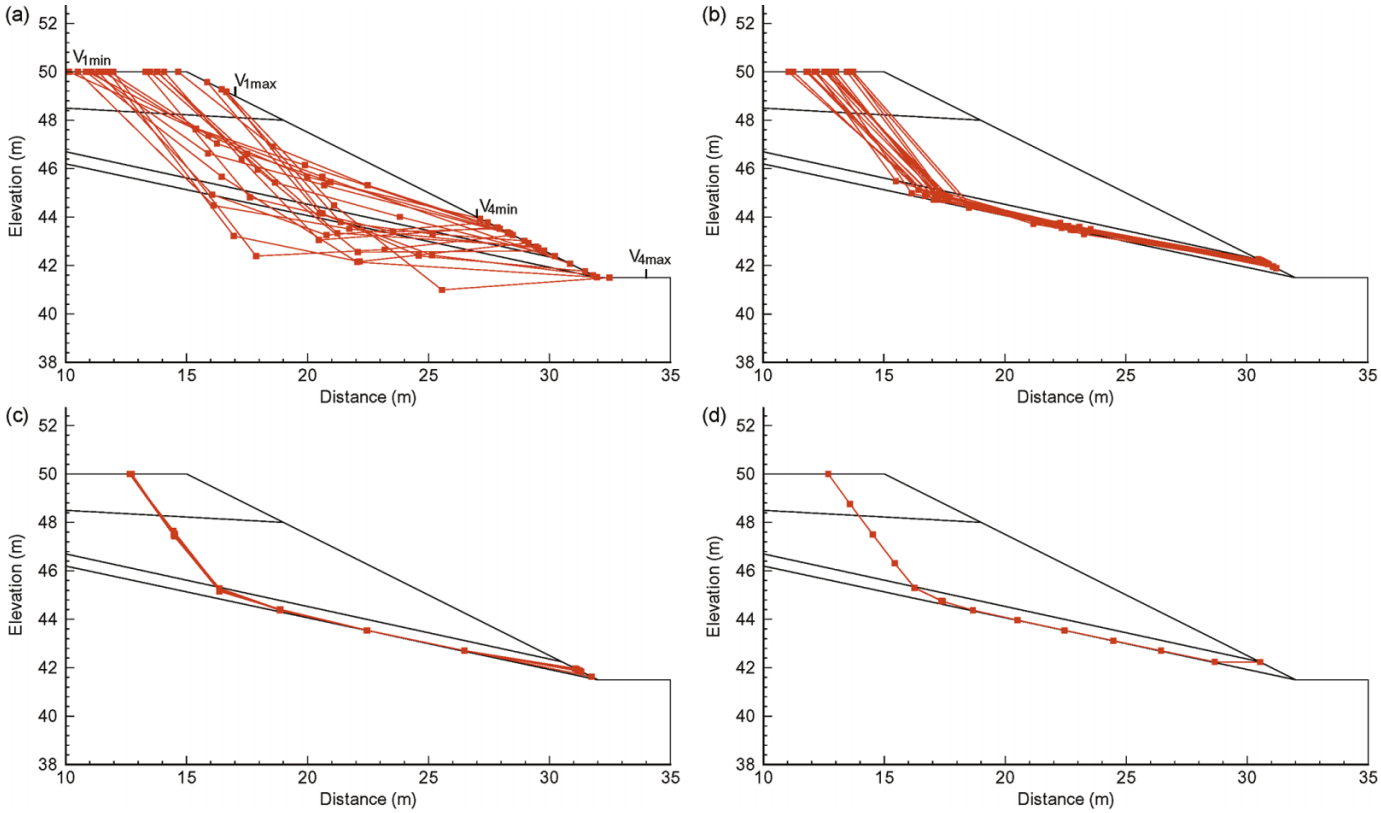


**Fig. 10.** Convergence process of the minimum factor of safety for example 2.

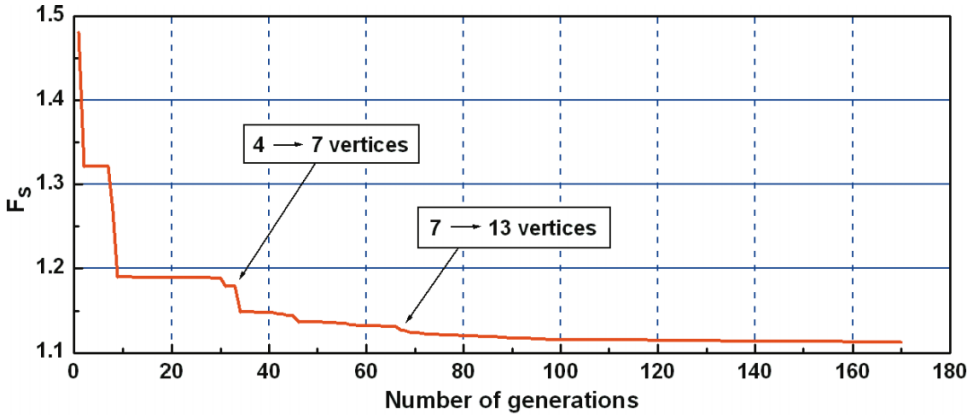


duced by Cheng et al. (2007) from 0.5 to 0.05 m to test the global search capacity of their approach to locate a localized weak layer. This modified problem is considered here as example 4. For analyses of this slope, in recognition of its particularly challenging nature, the number of initial slip surfaces generated in the proposed approach is doubled, i.e., $M_{slip} = 40$. The proposed approach considers 6640 slip surfaces to find the final solution for the analysis with the lowest $F_{s_{min}}$. A critical slip surface with an $F_{s_{min}}$ value of 1.197 is obtained, which is almost identical to that reported by Cheng et al., as shown in Fig. 11.

## Examples 5 and 6

Examples 5 and 6 were presented by Pham and Fredlund (2003) and are illustrated in Figs. 12 and 13, respectively. Pham and Fredlund investigated the use of the dynamic programming technique as a search algorithm. Following their approach, the finite-element-based method (Yamagami and Ueta 1988; Zou et al. 1995; Farias and Naylor 1998; Fredlund and Scoular 1999) is adopted to calculate $F_s$ for these examples. Before the search process, a linear elastic finite-element analysis is performed using Plaxis version 7.2 (Plaxis bv. 1998), with the soil properties presented by Pham and Fredlund (see Figs. 12, 13), using six-noded plane-strain triangular isoparametric elements. The stress field of the slope in the search domain is obtained by the superconvergent patch recovery technique (Zienkiewicz and Zhu 1992).

A slightly lower $F_{s_{min}}$ than that reported by Pham and Fredlund (2003) is obtained using the proposed approach for example 5, as listed in Table 3. Compared with the result

**Fig. 11.** Cross section and critical slip surfaces for example 4.

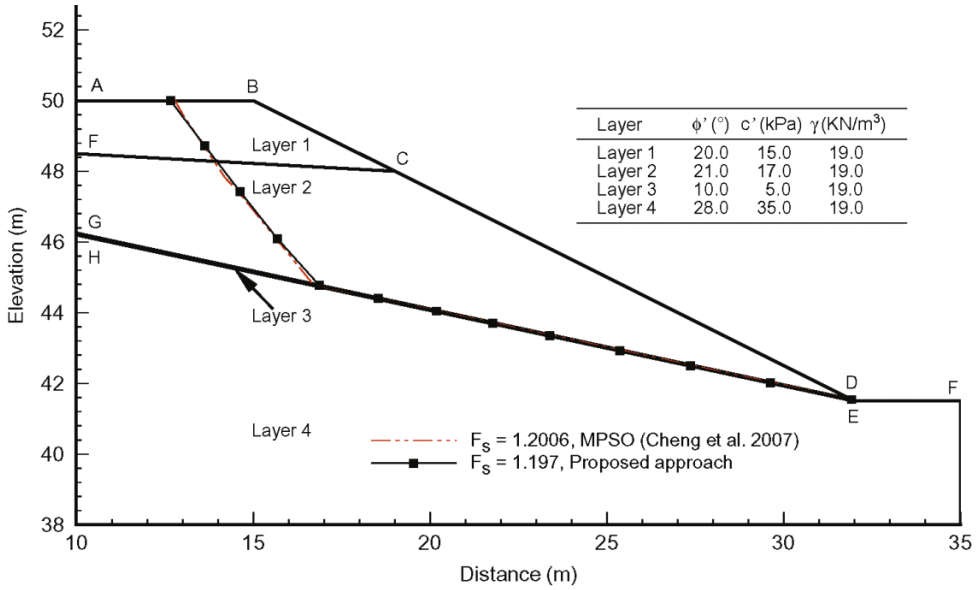


**Fig. 12.** Cross section and critical slip surfaces for example 5.

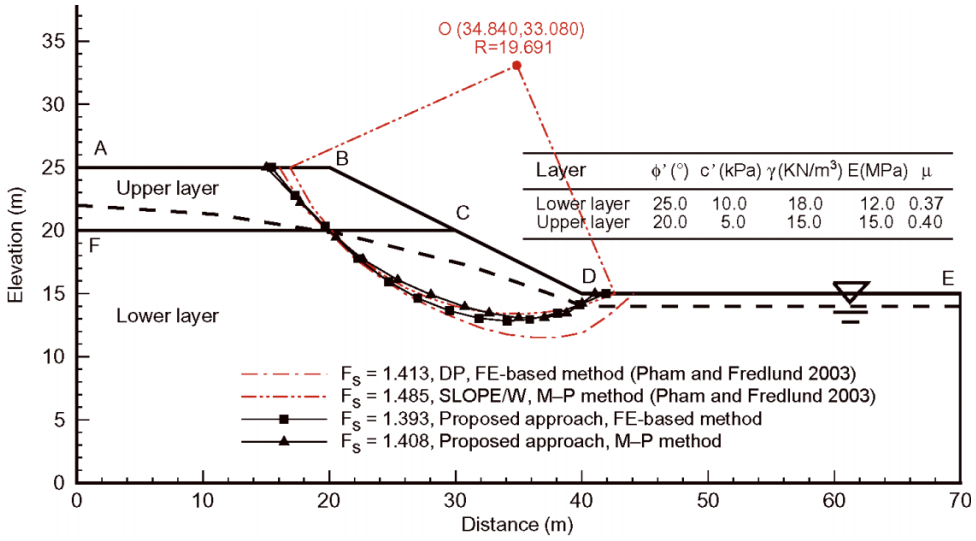


**Fig. 13.** Cross section and critical slip surfaces for example 6.

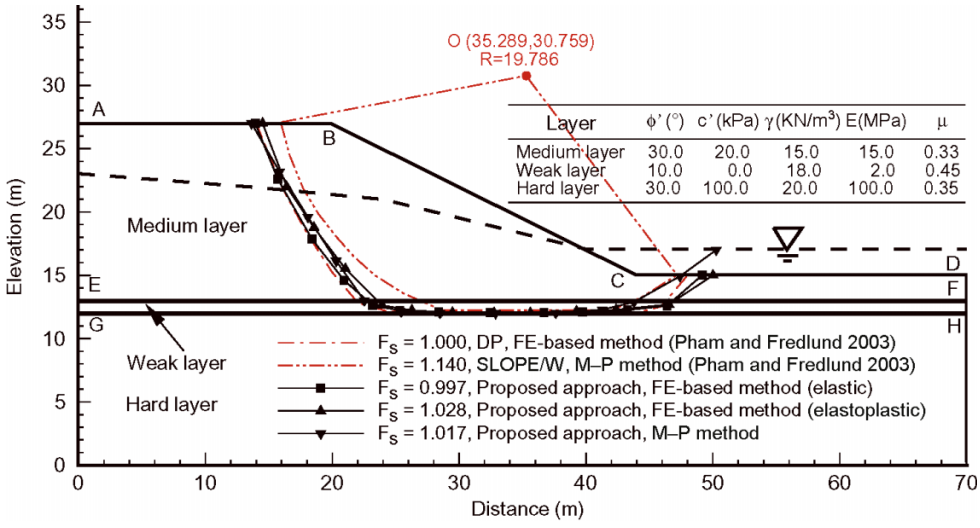

of Pham and Fredlund, the critical slip surface is shallower near the slope toe (in Fig. 12), which could be claimed to be more reasonable for a slope without a weak layer under the slope toe. This is confirmed by an additional analysis using the proposed search approach incorporating the Morgenstern–Price method, with the critical slip surfaces obtained by the proposed approach with two different methods of calculating $F_s$ being consistent. Furthermore, the critical slip surfaces are close to the SLOPE/W (GEO-SLOPE International Ltd. 2001) result reported by Pham and Fredlund, although slightly deeper in the part near the top of the slope.

The slope of example 6 is submerged in the downslope region, with one thin weak layer sandwiched between two relatively hard layers, as illustrated in Fig. 13. The weak layer is refined in the finite-element mesh, as the critical slip surface would be expected to pass through it. The proposed approach obtained a slightly lower $F_{s_{min}}$ than the dynamic programming result reported by Pham and Fredlund (2003), as listed in Table 3, and a strong correlation between the critical slip surfaces obtained by these two approaches is shown in Fig. 13. The proposed search approach is also used to analyze this problem incorporated with the Morgenstern–Price method regarding the impounded water at the slope toe as a no-strength material. Most of the upper part of the critical slip surface is similar to that of the two critical slip surfaces obtained by the finite-element-based method mentioned previously (Fig. 13), with a comparable $F_{s_{min}}$, but is shallower near the slope toe. As discussed by Pham and Fredlund (2003), this is because, unlike the finite-element-based method, limit equilibrium methods cannot take the stress concentration at the toe of the slope fully into account.

It is worth noting that a linear elastic finite-element analysis following that of Pham and Fredlund (2003) has been performed in example 6 to enable direct comparison of the proposed approach with the dynamic programming technique. However, plastic deformation might be expected to occur in the domain, particularly in the weak layer, since its $F_{s_{min}}$ value is approaching 1.0. Therefore, an additional analysis has been performed using the proposed approach with an elastoplastic finite-element analysis (Plaxis version 7.2, Plaxis bv. 1998). An $F_{s_{min}}$ value equal to 1.028 is obtained, which is 3.1% greater than that based on an elastic finite-element analysis, and the critical slip surfaces are in close agreement, as shown in Fig. 13.

It takes 3.47 and 4.74 s for the proposed approach to obtain the solutions for examples 5 and 6, respectively, with less than 2500 different possible slip surfaces considered. It should be acknowledged that, if the finite-element-based method is used, the computing time also depends on the finite-element mesh used. Here, meshes with 814 and 1904 six-noded triangular elements are employed for examples 5 and 6, respectively.

### Discussion

With the exception of example 1, all of the slopes presented in this paper are nonhomogeneous with relatively complex profiles. The proposed approach exhibits an excellent ability to locate noncircular critical slip surfaces for these challenging slopes. Furthermore, the proposed approach can obtain significantly improved solutions to examples 2 and 3 when compared with the simple binary GA (Zolfaghari et al. 2005), which failed to locate the critical slip surfaces. The results of this study allow alleviation of previously reported doubts on the applicability of the GA technique for locating noncircular critical slip surfaces (Sarma and Tan 2006; Cheng et al. 2007).

Although the number of different possible slip surfaces considered, which is a good indicator of efficiency, was only reported by a few researchers (Cheng 2003; Cheng et al. 2007) where comparisons are possible, the proposed approach is considerably more efficient than existing approaches. In particular, the modified particle swarm optimization technique (Cheng et al. 2007), although having the ability to find the converged solutions for complicated slopes, requires between 4 and 10 times the number of possible slip surfaces to be considered in examples 1, 2, and 3 and two times the number for the extremely challenging problem of example 4. In terms of computational time, it takes less than 10 s for the proposed approach to obtain a converged solution for the more complicated slopes considered in this paper on a computer easily available at present.

For each example investigated, three independent analyses of the proposed approach are performed. In each case, the values of $F_{s_{min}}$ for each of the three independent analyses are close to each other, as shown in Table 3, which demonstrates that the proposed approach is both stable and can be used to find a converged solution.

Limit equilibrium methods (Morgenstern and Price 1965; Spencer 1967) and the finite-element-based method (Yamagami and Ueta 1988; Zou et al. 1995; Farias and Naylor 1998; Fredlund and Scoular 1999) are incorporated successfully with the proposed approach. Furthermore, there is a strong correlation between the results of the analyses when various methods are used to assess $F_s$, as shown in examples 5 and 6.

Lastly, an alternative approach based on critical acceleration was proposed by Sarma and Tan (2006) to analyze examples 2 and 3 and obtained lower $F_{s_{min}}$ values. For instance, an $F_{s_{min}}$ values of 1.091 and a critical slip surface (Fig. 7) were obtained using this approach for example 2 which are obviously significantly different from the results of the proposed method and the modified particle swarm optimization approach (Cheng et al. 2007). An assumed tension crack in the analyses of Sarma and Tan with a depth of nearly 2.2 m at the slope top for both examples might be the primary reason for these lower values of $F_{s_{min}}$ and the different shapes of the critical slip surfaces.

## Conclusions

An efficient search approach based on the real-coded genetic algorithm has been developed to locate noncircular critical slip surfaces in slope stability analyses. Both limit equilibrium methods and the finite-element-based method are incorporated with the proposed search approach, and the results obtained using these two methods show good agreement. Geometrical and kinematical compatibility constraints, which are established based on the features of slope problems, prevent the consideration of unreasonable slip surfaces. A dynamic bound technique is developed to improve the search performance leading to a more effective exploration in the solution domain. Case studies demonstrate that the proposed search approach is both efficient in solving practical slope stability problems and capable of yielding highly accurate solutions. The proposed search approach is stable, and there is a strong correlation between the results of the proposed method

and those of independent analyses. Lastly, this paper clearly demonstrates that the genetic algorithm can be successfully applied to problems locating the noncircular critical slip surface.

Detailed data of the examples studied in this paper are presented in Tables B1 and C1 for completeness.

## Acknowledgement

This research project was supported by the National Natural Science Fund of China (NSFC) through grants 50425825, 50538080, and 50778163 and by the National Basic Research Program of China through grant 2007CB714200. Some of the work presented in this paper was carried out at the Centre for Engineering and Scientific Computation (CESC), Zhejiang University, and its director Prof. Y. Zheng is gratefully acknowledged.

## References

Arai, K., and Tagyo, K. 1985. Determination of noncircular slip surface giving the minimum factor of safety in slope stability analysis. Soils and Foundations, **25**(1): 43–51.

Baker, R. 1980. Determination of the critical slip surface in slope stability computations. International Journal for Numerical and Analytical Methods in Geomechanics, **4**(4): 333–359. doi:10.1002/nag.1610040405.

Bardet, J.P., and Kapuskar, M.M. 1989. A simplex analysis of slope stability. Computers and Geotechnics, **8**(4): 329–348. doi:10.1016/0266-352X(89)90039-6.

Bishop, A.W. 1955. The use of the slip circle in the stability analysis of slopes. Géotechnique, **5**(1): 7–17. doi:10.1680/geot.1955.5.1.7.

Boutrup, E., and Lovell, C.W. 1980. Search techniques in slope stability analysis. Engineering Geology, **16**(1–2): 51–61. doi:10.1016/0013-7952(80)90006-X.

Celestino, T.B., and Duncan, J.M. 1981. Simplified search for noncircular slip surfaces. *In* Proceedings of the 10th International Conference on Soil Mechanics and Foundation Engineering, Stockholm, Sweden, 15–19 June 1981. A.A. Balkema, Rotterdam, the Netherlands. Vol. 3, pp. 391–394.

Chen, Z.-Y. 1992. Random trials used in determining global minimum factors of safety of slopes. Canadian Geotechnical Journal, **29**(2): 225–233. doi:10.1139/t92-026.

Chen, Z.-Y., and Shao, C.-M. 1988. Evaluation of minimum factor of safety in slope stability analysis. Canadian Geotechnical Journal, **25**(4): 735–748. doi:10.1139/t88-084.

Cheng, Y.M. 2003. Location of critical failure surface and some further studies on slope stability analysis. Computers and Geotechnics, **30**(3): 255–267. doi:10.1016/S0266-352X(03)00012-.

Cheng, Y.M., Li, L., Chi, S., and Wei, W.B. 2007. Particle swarm optimization algorithm for the location of the critical non-circular failure surface in two-dimensional slope stability analysis. Computers and Geotechnics, **34**(2): 92–103. doi:10.1016/j.compgeo.2006.10.012.

de Jong, K.A. 1975. An analysis of the behavior of a class of genetic adaptive systems. University of Michigan, Ann Arbor, Mich.

Eiben, A.E., and Smith, J.E. 2003. Introduction to evolutionary computing. Springer-Verlag, Berlin, Germany.

Farias, M.M., and Naylor, D.J. 1998. Safety analysis using finite elements. Computers and Geotechnics, **22**(2): 165–181. doi:10.1016/S0266-352X(98)00005-6.

Fredlund, D.G., and Scoular, R.E.G. 1999. Using limit equilibrium in finite element slope stability analysis. *In* IS-Shikoku'99: Proceedings of the International Symposium on Slope Stability Engineering, Matsuyama, Japan, 8–11 November 1999. *Edited by* J.C. Jiang, Y. Norio, and T. Yamagami. A.A. Balkema, Rotterdam, the Netherlands. pp. 31–47.

GEO-SLOPE International Ltd. 2001. SLOPE/W user's manual, version 4.0. GEO-SLOPE International Ltd., Calgary, Alta.

Goh, A.T.C. 1999. Genetic algorithm search for critical slip surface in multiple-wedge stability analysis. Canadian Geotechnical Journal, **36**(2): 382–391. doi:10.1139/cgj-36-2-382.

Goldberg, D.E., and Deb, K. 1991. A comparative analysis of selection schemes used in genetic algorithms. *In* Proceedings of the 1st Workshop on the Foundations of Genetic Algorithms, Bloomington, Ind., 15–18 July 1990. *Edited by* G.J.E. Rawlins. Morgan Kaufmann, San Mateo, Calif. pp. 69–93.

Greco, V.R. 1996. Efficient Monte Carlo technique for locating critical slip surface. Journal of Geotechnical Engineering, ASCE, **122**(7): 517–525. doi:10.1061/(ASCE)0733-9410(1996)122:7(517).

Holland, J. 1975. Adaptation in natural and artificial systems. University of Michigan Press, Ann Arbor, Mich.

Hrstka, O., and Kucerova, A. 2004. Improvements of real coded genetic algorithms based on differential operators preventing premature convergence. Advances in Engineering Software, **35**(3–4): 237–246. doi:10.1016/S0965-9978(03)00113-3.

Husein Malkawi, A.I., Hassan, W.F., and Sarma, S.K. 2001*a*. An efficient search method for finding the critical circular slip surface using the Monte Carlo technique. Canadian Geotechnical Journal, **38**(5): 1081–1089. doi:10.1139/cgj-38-5-1081.

Husein Malkawi, A.I., Hassan, W.F., and Sarma, S.K. 2001*b*. Global search method for locating general slip surface using Monte Carlo techniques. Journal of Geotechnical and Geoenvironmental Engineering, ASCE, **127**(8): 688–698. doi:10.1061/(ASCE)1090-0241(2001)127:8(688).

Janbu, N. 1954. Application of composite slip surfaces for stability analysis. *In* Proceedings of the European Conference on Stability of Earth Slopes. Stockholm, Sweden. Vol. 3, pp. 43–49.

Li, K.S., and White, W. 1987. Rapid evaluation of the critical slip surface in slope stability problems. International Journal for Numerical and Analytical Methods in Geomechanics, **11**(5): 449–473. doi:10.1002/nag.1610110503.

McCombie, P., and Wilkinson, P. 2002. The use of the simple genetic algorithm in finding the critical factor of safety in slope stability analysis. Computers and Geotechnics, **29**(8): 699–714. doi:10.1016/S0266-352X(02)00027-7.

Menon, D., Nair, K.K., and Gandhi, S.R. 2001. Reliability analysis of excavation slips in clayey soils. *In* Proceedings of the 2001 Mechanics and Materials Summer Conference, San Diego, Calif., 27–29 June 2001. ASCE, New York. pp. 79–93.

Morgenstern, N.R., and Price, V.E. 1965. The analysis of the stability of general slip surfaces. Géotechnique, **15**(1): 79–93. doi:10.1680/geot.1965.15.1.79.

Narayan, C.G.P., Bhatkar, V.P., and Ramamurthy, T. 1982. Nonlocal variational method in stability analysis. Journal of the Geotechnical Engineering Division, ASCE, **108**(11): 1443–1459.

Pham, H.T.V., and Fredlund, D.G. 2003. The application of dynamic programming to slope stability analysis. Canadian Geotechnical Journal, **40**(4): 830–847. doi:10.1139/t03-033.

Plaxis bv. 1998. Plaxis finite element code for soil and rock analyses, version 7. Plaxis bv., AN Delft, the Netherlands.

Sarma, S.K. 1973. Stability analysis of embankments and slopes. Géotechnique, **23**(3): 423–433. doi:10.1680/geot.1973.23.3.423.

Sarma, S.K. 1979. Stability analysis of embankments and slopes. Journal of Geotechnical Engineering, ASCE, **105**(12): 1511–1524.

Sarma, S.K., and Tan, D. 2006. Determination of critical slip surface in slope analysis. Géotechnique, **56**(8): 539–550. doi:10.1680/geot.2006.56.8.539.

Siegel, R.A., Kovacs, W.D., and Lovell, C.W. 1981. Random sur-

face generation in stability analysis. Journal of the Geotechnical Engineering Division, ASCE, **107**(7): 996–1002.

Spencer, E. 1967. A method for analysis of the stability of embankments assuming parallel interslice forces. Géotechnique, **17**(1): 11–26. doi:10.1680/geot.1967.17.1.11.

Yamagami, T., and Ueta, Y. 1988. Search for noncircular slip surface by the Morgenstern–Price method. *In* Proceedings of the 6th International Conference on Numerical Methods in Geomechanics, Innsbruck, Austria, 11–15 April 1988. *Edited by* G. Swoboda. A.A Balkema, Rotterdam, the Netherlands. pp. 1219–1223.

Zhu, D.-Y. 2001. A method for locating critical slip surfaces in slope stability analysis. Canadian Geotechnical Journal, **38**(2): 328–337. doi:10.1139/cgj-38-2-328.

Zhu, D.Y., Lee, C.F., Qian, Q.H., and Chen, G.R. 2005. A concise algorithm for computing the factor of safety using the Morgenstern–Price method. Canadian Geotechnical Journal, **42**(1): 272–278. doi:10.1139/t04-072.

Zienkiewicz, O.C., and Zhu, J.Z. 1992. The superconvergent patch recovery (SPR) and adaptive finite-element refinement. Computer Methods in Applied Mechanics and Engineering, **101**(1–3): 207–224. doi:10.1016/0045-7825(92)90023-D.

Zolfaghari, A.R., Heath, A.C., and McCombie, P.F. 2005. Simple genetic algorithm search for critical non-circular failure surface in slope stability analysis. Computers and Geotechnics, **32**(3): 139–152. doi:10.1016/j.compgeo.2005.02.001.

Zou, J.-Z., Williams, D.J., and Xiong, W.-L. 1995. Search for critical slip surfaces based on finite element method. Canadian Geotechnical Journal, **32**(2): 233–246. doi:10.1139/t95-026.

## List of symbols

| | |
|---|---|
| $a_i$ | real variable in a solution representation in real-coded GA |
| $a_{k_{\min}}$, $a_{k_{\max}}$ | lower and upper boundaries for variable $a_k$, respectively |
| $\boldsymbol{A}^j$ | real-value solution to a continuous optimization problem |
| $\boldsymbol{A}^{j'}$ | solution after mutation |
| $\boldsymbol{A}^p$, $\boldsymbol{A}^q$ | solution before crossover |
| $\boldsymbol{A}^{p'}$, $\boldsymbol{A}^{q'}$ | solution after crossover |
| $c$, $c'$ | cohesion |
| $E$ | elastic modulus |
| $F_s$ | factor of safety |
| $F_{s_{\min}}$ | minimum factor of safety |
| $i_{gen}$ | current generation number |
| $j$ | serial number of individual solution |
| $k_{i,j}$ | slope of the line connecting $V_i$ and $V_j$ |
| $M_{add}$ | number of generations at which additional vertices can be added |
| $M_{NI\_add}$ | maximum number of generations allowed for adding vertices with no improvement in solution fitness |
| $M_{NI\_term}$ | maximum number of generations allowed with no improvement in fitness before termination of search |
| $M_{slip}$ | number of slip surfaces in real-coded GA |
| $M_{term}$ | minimum number of generations before termination of search is allowed |
| $M_{vtx}$ | number of vertices defining slip surface |
| $n$ | number of variables for a real-value solution |
| O | centre of circular slip surface |
| $r_{crs}$ | probability for crossover operator in GA |
| $r_{mut}$ | probability for mutation operator in GA |
| $R$ | radius of circular slip surface |
| $\boldsymbol{s}_i$ | $i$ vertex vector for describing a slip surface |
| $V_j$ | vertex of a slip surface |
| $V_j^s$ | vertex of the slope surface |
| $(x_i, y_i)$ | coordinates of $V_i$ |
| $(x_j^s, y_j^s)$ | coordinates of $V_j^s$ |
| $x_{i_{\min}}$, $x_{i_{\max}}$ | lower and upper $x$ ordinate boundaries for $V_i$ |
| $y_{i_{\min}}$, $y_{i_{\max}}$ | lower and upper $y$ ordinate boundaries for $V_i$ |
| $\alpha_i$ | inclined angle of the $i$th segment of the slip surface |
| $\varepsilon_{add}$ | specified relative difference for adding vertices |
| $\varepsilon_{term}$ | specified relative difference for terminating search approach |
| $\eta$ | parameter for controlling crossover rate |
| $\gamma$ | soil unit weight |
| $\mu$ | Poisson's ratio |
| $\phi$, $\phi'$ | friction angle |

## Appendix A

The pseudo-algorithm for the proposed real-coded GA approach is illustrated in Fig. A1.

**Fig. A1.** Pseudo-algorithm for the real-coded GA search approach.

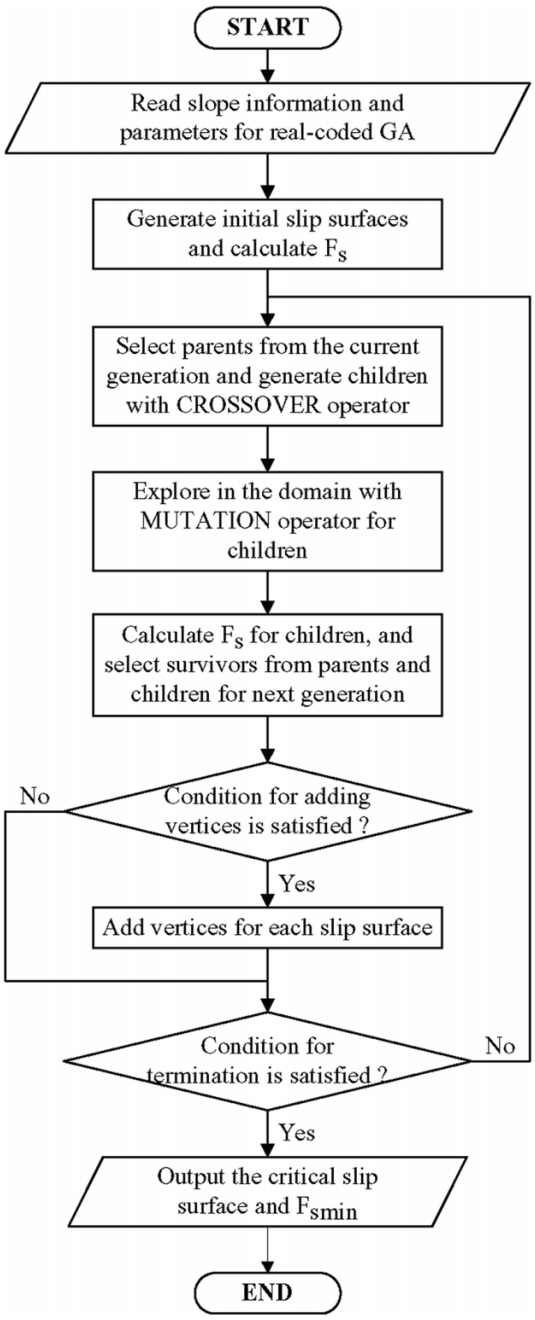

## Appendix B

A summary of the coordinates for the vertices of the geological layers and phreatic lines of the examples is given in Table B1.

**Table B1.** Coordinates for the vertices of geological layers and phreatic line of examples 1–6.

| Vertex No. | Example 1 | Example 2 | Example 3 | Example 4 | Example 5 | Example 6 |
|---|---|---|---|---|---|---|
| **Geological layers** | | | | | | |
| A | (0.00, 5.00) | (10.00, 50.00) | (10.00, 50.00) | (10.00, 50.00) | (0.00, 25.00) | (0.00, 27.00) |
| B | (5.00, 5.00) | (15.00, 50.00) | (15.00, 50.00) | (15.00, 50.00) | (20.00, 25.00) | (20.00, 27.00) |
| C | (15.00, 10.00) | (19.00, 48.00) | (19.00, 48.00) | (19.00, 48.00) | (30.00, 20.00) | (44.00, 15.00) |
| D | (25.00, 10.00) | (30.50, 42.25) | (25.00, 45.00) | (31.90, 41.55) | (40.00, 15.00) | (70.00, 15.00) |
| E | — | (32.00, 41.50) | (27.00, 44.00) | (32.00, 41.50) | (70.00, 15.00) | (0.00, 13.00) |
| F | — | (35.00, 41.50) | (32.00, 41.50) | (35.00, 41.50) | (0.00, 20.00) | (70.00, 13.00) |
| G | — | (10.00, 48.50) | (40.00, 41.50) | (10.00, 48.50) | — | (0.00, 12.00) |
| H | — | (10.00, 46.70) | (10.00, 48.10) | (10.00, 46.25) | — | (70.00, 12.00) |
| I | — | (10.00, 46.20) | (10.00, 45.00) | (10.00, 46.20) | — | — |
| J | — | — | (10.00, 44.00) | — | — | — |
| **Phreatic line** | | | | | | |
| | | | | | (0.00, 22.00) | (0.00, 23.00) |
| | | | | | (10.87, 21.28) | (14.00, 22.00) |
| | | | | | (21.14, 19.68) | (24.00, 21.00) |
| | | | | | (31.21, 17.17) | (40.00, 17.00) |
| | | | | | (38.69, 14.56) | (70.00, 17.00) |
| | | | | | (40.00, 14.00) | |
| | | | | | (70.00, 14.00) | |

## Appendix C

A summary of the coordinates for the 13 vertex critical slip surfaces of the six examples is given in Table C1.

**Table C1.** Coordinates for the 13 vertex critical slip surfaces of examples 1–6.

| Vertex No. | Example 1 | Example 2 | Example 3 | Example 4 | Example 5 | Example 6 |
|---|---|---|---|---|---|---|
| 1 | (4.60, 5.00) | (30.53, 42.23) | (26.92, 44.04) | (31.91, 41.54) | (41.89, 15.00) | (49.14, 15.00) |
| 2 | (5.39, 4.53) | (28.66, 42.24) | (25.53, 44.01) | (29.63, 42.01) | (39.83, 14.12) | (46.38, 12.59) |
| 3 | (6.23, 4.18) | (26.44, 42.70) | (23.76, 44.00) | (27.37, 42.49) | (38.09, 13.46) | (43.27, 12.25) |
| 4 | (7.30, 3.96) | (24.46, 43.12) | (21.38, 44.01) | (25.37, 42.92) | (35.87, 12.95) | (39.70, 12.10) |
| 5 | (8.39, 3.90) | (22.45, 43.55) | (20.46, 44.02) | (23.38, 43.35) | (34.07, 12.83) | (36.69, 12.05) |
| 6 | (9.56, 4.00) | (20.50, 43.97) | (19.30, 44.09) | (21.78, 43.70) | (31.85, 13.05) | (32.45, 12.07) |
| 7 | (10.78, 4.23) | (18.66, 44.37) | (18.32, 44.29) | (20.17, 44.05) | (29.54, 13.63) | (28.38, 12.10) |
| 8 | (12.16, 4.68) | (17.39, 44.75) | (17.40, 44.58) | (18.53, 44.41) | (27.01, 14.63) | (25.33, 12.23) |
| 9 | (13.36, 5.28) | (16.25, 45.30) | (16.46, 45.00) | (16.87, 44.77) | (24.70, 15.95) | (23.19, 12.61) |
| 10 | (14.70, 6.19) | (15.43, 46.31) | (15.38, 46.21) | (15.68, 46.10) | (22.24, 17.77) | (20.92, 14.61) |
| 11 | (16.04, 7.32) | (14.52, 47.51) | (14.33, 47.57) | (14.62, 47.42) | (19.67, 20.33) | (18.38, 17.89) |
| 12 | (17.33, 8.62) | (13.58, 48.76) | (13.45, 48.77) | (13.62, 48.72) | (17.28, 22.77) | (15.71, 22.58) |
| 13 | (18.53, 10.00) | (12.68, 50.00) | (12.58, 50.00) | (12.65, 50.00) | (15.41, 25.00) | (13.92, 27.00) |